

Cite this: *RSC Adv.*, 2019, 9, 18439

Micranthanosides I and II, two novel 1,10-secograyanane diterpenoids and their antinociceptive analogues from the leaves and twigs of *Rhododendron micranthum*†

Yuxun Zhu,‡ Huimin Yan,‡ Xiaojing Wang, Zhaoxin Zhang, Huanping Zhang, Lisha Chai, Li Li, Jing Qu and Yong Li *

Micranthanosides I and II (1–2), two diterpenoid glucosides featuring a new 1,10-secograyanane skeleton, thirteen new diterpenoid glycosides (3–15), and 21 known analogues were obtained from the ethanol extract of the leaves and twigs of *Rhododendron micranthum*. Micranthanoside XII (12) represent the first example of 3,5-epoxy-4,5-seco-*ent*-kaurane diterpenoid. The structures of these compounds were determined by spectroscopic data analysis and quantum chemical calculations. To clarify the chemical basis and provide reference for rational use of this medicinal plant, the antinociceptive and the anti-inflammatory activities of the compounds were tested. In the acetic acid-induced writhing test, compounds 17 and 19 showed significant antinociceptive activity at a dose of 3 mg kg⁻¹ and compounds 2, 6 and 32 showed significant antinociceptive activity at a dose of 10 mg kg⁻¹. Toxic reactions such as nausea and convulsion were observed when 17, 19, 29, and 31 at a dose of 10 mg kg⁻¹ or 30 and 33 at a dose of 1 mg kg⁻¹ were administered. The anti-inflammatory activities of the isolated compounds were evaluated by measuring the inhibitory effects of LPS-induced NO production in BV2 cells. At 10 μM, micranthanoside IX (9) and rhodomicranoside F (26) showed moderate anti-inflammatory activities with inhibition rates of 56.31% and 72.43%, respectively.

Received 7th March 2019
Accepted 22nd May 2019

DOI: 10.1039/c9ra01736d

rsc.li/rsc-advances

Introduction

Natural products have been important sources for drug discovery.^{1,2} Evidence suggests that natural products continue to play a significant role in the area of genomics.³ *Rhododendron micranthum* Turcz. (Ericaceae), commonly known as “zhaoshanbai”, is widely distributed in northern China. This plant is used traditionally as a medicine for the treatment of post-partum arthralgia and chronic bronchitis.⁴ The extract of *R. micranthum* has also been developed as a drug for clinical use. Meanwhile, cases of clinical poisoning with “zhaoshanbai” have occasionally been reported.^{5,6} In these cases, some patients were found to have side effects and toxic symptoms such as nausea, epigastric pain and burning, hypotension, bradycardia, and dizziness.⁷ Although andromedotoxin from *R. micranthum* has been reported to be toxic,⁸ the chemical basis of its

antinociceptive and anti-inflammatory effects as well as its toxicity is still not well understood.

Previously, we have reported antinociceptive grayanane diterpenoids with structural diversity from *R. molle*, *R. decorum*, and *Pieris formosa*. Among them, rhodojaponin III and VI, craiobiotoxin IX, and pieristoxin N and P were found to be highly potent in several antinociceptive models.^{9–12} In addition, micranthanoside A, grayanotoxins I, and III in *R. micranthum* were reported to have significant antinociceptive activity at a dose of 0.2 mg kg⁻¹ in the acetic acid-induced writhing test.^{13,14} In order to provide chemical evidence for rational application of “zhaoshanbai” and discover structurally interesting lead compounds, leaves and twigs of *R. micranthum* (107.5 kg) were collected from Shandong Province. An ethanol extract of the leaves and twigs of *R. micranthum* was investigated and afforded 36 diterpenoids, including 15 new analogues (1–15) (Fig. 1). The isolation, structural elucidation, antinociceptive activities, and anti-inflammatory activities of these compounds are described herein.

Results and discussion

Compound 1 (micranthanoside I) was obtained as white powder and was found to have a molecular formula of C₂₆H₄₂O₈ based

State Key Laboratory of Bioactive Substance and Function of Natural Medicines, Institute of Materia Medica, Chinese Academy of Medical Sciences, Peking Union Medical College, Beijing 100050, People's Republic of China. E-mail: liyong@imm.ac.cn

† Electronic supplementary information (ESI) available: 1D and 2D NMR, HRESIMS, CD, GC analysis, and IR. See DOI: 10.1039/c9ra01736d

‡ Y.-X. Z. and H.-M. Y. contributed equally.



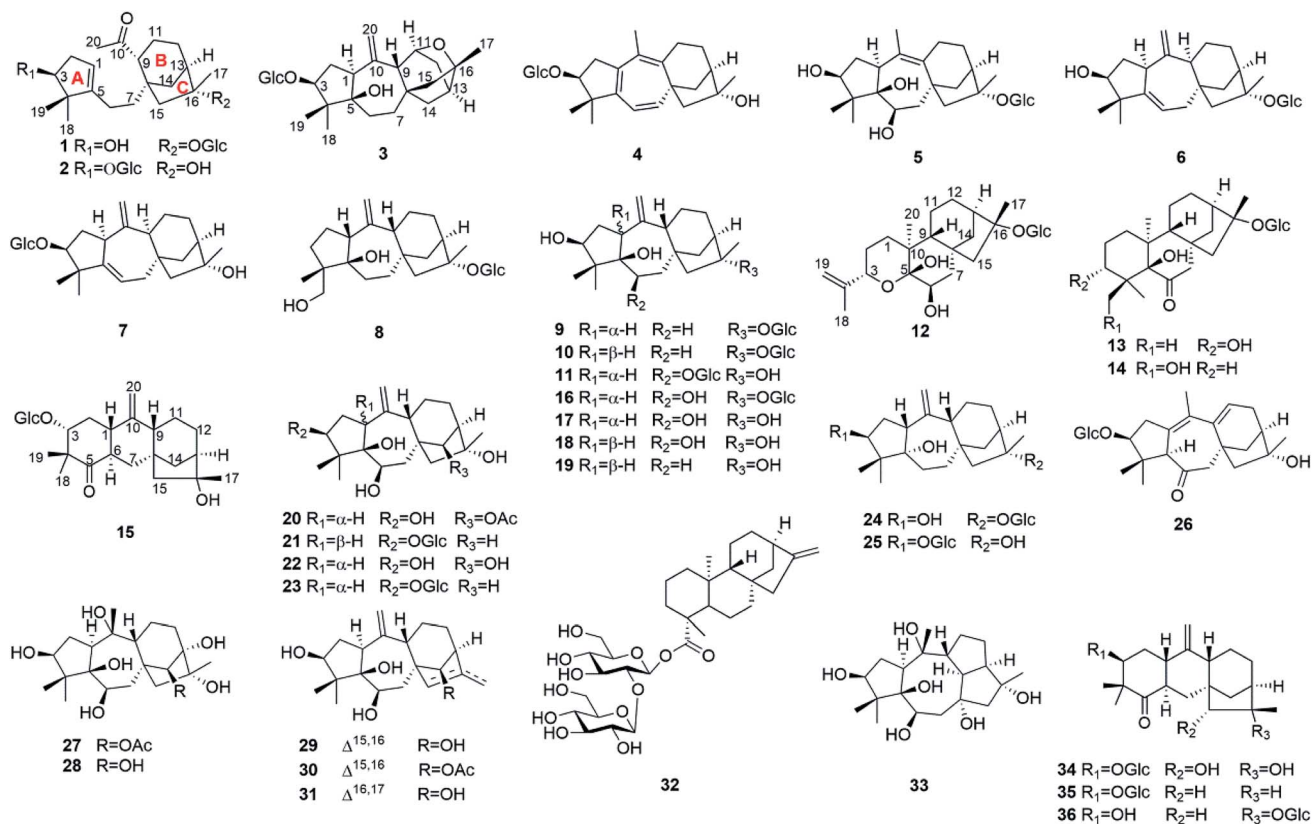


Fig. 1 Chemical structures of compounds 1–36.

on the (+)-HRESIMS ion at m/z 505.2786 $[M + Na]^+$ (calcd. for $C_{26}H_{42}O_8Na$, 505.2772), corresponding to six indices of hydrogen deficiency (IHD). Its IR spectrum suggested the presence of hydroxy (3368 cm^{-1}) and carbonyl (1700 cm^{-1}) functionalities. The 1H NMR (Table 1) data showed resonances of four methyl groups (δ_H 1.20, 1.28, 1.64, and 2.17), a glucose unit (δ_H 3.93, 3.97, 4.24, 4.25, 4.38, 4.51, and 5.01), and an olefinic proton at δ_H 5.27. The ^{13}C NMR data (Table 4), HSQC, and DEPT spectra of **1** exhibited 26 carbon resonances, including four methyls, eight methylenes, nine methines, and five sp^3 carbons. A sugar unit, a carbonyl group, and a double bond account for three of the IHDs, which suggest that the remaining part is consisting of three rings.

The COSY (Fig. 2a) and HSQC spectra established four fragments: $CH(OH)-CH_2-CH$, CH_2-CH_2 , $CH-CH_2-CH_2-CH-CH_2$, and $CH-CH(OH)-CH(OH)-CH(OH)-CH-CH_2(OH)$. Fragment a and the HMBC correlations from two *gem*-dimethyl singlets (H_3-18 and H_3-19) to carbons C-3, C-4, and C-5 allowed the five-membered carbon ring (ring A in Fig. 1) to be defined. The HMBC correlations from H-6 to C-1 and from H_2-7 to C-5 connected C-5 directly to fragment b *via* C-6. HMBC correlations from H-9 and H-14 (two ends of fragment c) to δ_C 47.3 (C-8), from H_2-12 to quaternary carbon at δ_C 88.1 (C-16), as well as correlations from H_2-15 to C-8, C-9, C-14, and C-16 revealed a bicyclo[3.2.1]octane ring system (rings B/C). The HMBC correlations from H_3-20 (δ_H 2.17) to C-9 (δ_C 53.6)/C-10 (δ_C 212.9) indicated that C-9 was connected to C-10. Finally, key HMBC

correlations from H-1 to C-6 and from H-9 and H_2-15 to C-7 confirmed the connection of C-5 and C-8 *via* fragment b. The glucose unit was placed at C-16 based on the HMBC correlation from H-1' to C-16. As a result, the planar structure of **1** was fully established, which is the first example of a 1,10-secograyanane.

The relative configuration of **1** was deduced by the NOESY experiments. Ring A and rings B/C were connected through two methylenes, which should theoretically provide molecular flexibility and complicate the stereochemical analysis. The NOESY correlations of $H_3-18/H-6\alpha$ and $H-14\alpha/H-7\alpha$ (α -side) and $H_3-19/H-6\beta$ and $H-14\beta/H-7\beta$ (β -side) indicated that bulky substituents at C-5 and C-8 restrict the rotation of the C-6/C-7 bond and led to a preferential conformation in pyridine- d_5 (room temperature) in which C-5 and C-8 were in the anti-position (Fig. 2b). The NOESY correlations of $H-3/H_3-18$, $H_3-18/H-6\alpha$, $H_3-19/H-6\beta$, $H-6\beta/H-9$, $H-9/H-15\beta$, and $H_3-17/H-12\beta$ indicated that H-3 is α -oriented and H-9 and CH_3-17 are β -oriented. The anomeric proton at H-1' (δ_H 5.01) showed a large coupling constant (7.8 Hz), indicating that the glucose unit is in β -configuration. Acid hydrolysis and GC analysis of the sugar moiety of **1** confirmed that the sugar was D-glucose (retention time: 29.35 min). To determine the absolute configuration of **1**, the ECD spectra for **1a** (3*S*,8*S*,9*R*,13*R*,16*R*,1'*S*,2'*R*,3'*S*,4'*S*,5'*R*) and its enantiomer **1b** were calculated using time-dependent density functional theory calculations at the B3LYP/6-31+G(d,p) level in methanol.¹⁵ The measured CD spectrum of **1** agreed well with the calculated ECD



Table 1 ^1H NMR spectroscopic data for compounds 1–7 in pyridine- d_5 (δ in ppm, J in Hz)

No	1 ^a	2 ^b	3 ^b	4 ^b	5 ^b	6 ^a	7 ^a
1	5.27, brs	5.16, brs	3.39, m	—	3.51, t (9.4)	3.34, d (8.5)	3.29, d (9.3)
2	2.46, m	2.55, m	2.33, m	2.87, dd (16.1, 6.8)	2.41, m	2.19, m	2.38, m
	2.64, dd, (15.3, 6.7)	2.69, dd (14.1, 7.1)	2.63, m	3.34, dd (16.2, 7.3)	2.41, m	2.41, m	2.57, m
3	4.26, m	4.24, t (7.2)	4.2, m	4.35, t (7.0)	3.87, m	4.38, brs	4.40, m
4	—	—	—	—	—	—	—
5	—	—	—	—	—	—	—
6	2.07, m	2.00, m	1.62, m	6.07, d (9.8)	4.25, m	5.36, brs	5.51, m
	2.29, t (13.5)	2.15, m	1.73, m	—	—	—	—
7	1.78, m	1.65, m	1.24, d (11.1)	5.55, d (9.8)	2.39, m	2.40, m	2.18, m
	1.91, m	1.88, m	2.11, m	—	2.53, m	2.52, m	2.51, m
8	—	—	—	—	—	—	—
9	2.76, brs	2.73, d (7.2)	2.90, brs	—	—	2.18, m	2.15, m
10	—	—	—	—	—	—	—
11	1.57, m	1.59, m	4.38, m	2.20, m	2.10, m	1.73, m	1.72, m
	1.59, m	1.66, m	—	2.45, dd (15.0, 7.1)	2.61, dd (15.2, 6.5)	1.73, m	1.82, m
12	1.55, m	1.58, m	1.64, m	1.79, m	1.54, m	1.48, m	1.52, m
	1.92, m	1.91, m	1.84, m	1.88, m	1.70, m	1.72, m	1.54, m
13	2.53, brs	2.19, brs	2.19, t (6.6)	2.32, m	2.54, brs	2.47, brs	2.15, m
14	2.36, m	2.30, dd (11.0, 4.7)	1.41, m	2.13, d (11.0)	1.58, d (10.8)	1.55, d (11.1)	1.62, d (10.1)
	2.38, m	2.43, d (11.2)	1.98, dd (11.7, 3.3)	2.39, dd (11.0, 4.7)	2.71, m	2.23, m	2.14, m
15	1.55, m	1.67, d (14.0)	1.24, d (11.1)	1.60, d (12.2)	2.41, m	1.74, d (12.8)	1.92, brs
	2.37, m	2.04, d (13.8)	1.79, dd (11.1, 3.3)	2.09, d (12.5)	2.90, d (15.2)	2.26, d (14.2)	1.92, brs
16	—	—	—	—	—	—	—
17	1.64, s	1.58, s	1.43, s	1.39, s	1.67, s	1.59, s	1.54, s
18	1.20, s	1.21, s	0.99, s	1.34, s	0.88, s	1.17, s	1.28, s
19	—	—	—	—	—	—	—
19	1.28, s	1.27, s	1.48, s	1.31, s	1.32, s	1.22, s	1.28, s
20	2.17, s	2.15, s	5.05, s	1.79, s	1.84, s	4.96, s	5.00, s
	—	—	5.47, s	—	—	5.09, s	5.20, s
1'	5.01, d (7.8)	4.70, d (7.8)	4.99, d (7.8)	5.03, d (7.8)	5.05, d (7.8)	5.01, d (7.8)	5.04, d (7.8)
2'	3.97, m	4.05, m	3.99, m	4.07, brs	4.00, m	4.01 t, (11.1)	4.06, m
3'	4.25, m	4.28, m	4.27, m	4.28, m	4.28, m	4.29, m	4.29, m
4'	4.24, m	4.28, m	4.23, m	4.27, m	4.29, m	4.26, m	4.29, m
5'	3.93, brs	3.97, brs	4.02, m	4.02, brs	3.90, m	3.94, brs	4.03, m
6'	4.38, dd (11.6, 5.1)	4.42, dd (11.7, 5.2)	4.42, m	4.42, d (11.8)	4.39, m	4.36, m	4.45, m
	4.51, dd (11.6, 2.6)	4.58, dd (11.7, 2.4)	4.61, d (11.9)	4.60, d (11.5)	4.49, d (10.6)	4.51, d (11.3)	4.62, d (9.6)

^a Recorded at 500 MHz. ^b Recorded at 600 MHz.

of **1a** and is the opposite of that of **1b** (Fig. 3). Thus, the absolute configuration of **1** was established.

Compound **2** (micranthanoside II) was obtained as white powder and was found to have a molecular formula of $\text{C}_{26}\text{H}_{42}\text{O}_8$. Its NMR data were highly similar to those of **1** except for the variations in the chemical shifts of C-3 ($\Delta\delta_{\text{C}} +8.3$) and C-16 ($\Delta\delta_{\text{C}} -8.9$), suggesting that the glucose unit was placed at C-3. The key HMBC correlation from H-1' to C-3 confirmed the above assignment. The relative configuration of **2** was assigned the same as **1** by its NOESY correlations of H-3/H₃-18 and H-9/H-15 β . The anomeric proton at H-1' (δ_{H} 4.70) showed a large coupling constant (7.8 Hz), indicating that the glucose unit is in β -configuration. Acid hydrolysis and GC analysis of the sugar moiety of **2** confirmed that the sugar was D-glucose (retention time: 29.32 min). The CD spectrum of **2** was consistent with that of **1**, showing a negative cotton effect at 303 nm (ESI Fig. S163 and S164[†]). Thus, the absolute configuration of **2** was assigned as (3*S*,8*S*,9*R*,13*R*,16*R*,1'*R*,2'*R*,3'*S*,4'*S*,5'*R*).

Compound **3** (micranthanoside III) has a molecular formula of $\text{C}_{26}\text{H}_{40}\text{O}_8$ based on the HRESIMS data, which suggested seven indices of hydrogen deficiency (IHD). The ^1H -NMR data showed resonances of three methyl groups (δ_{H} 0.99, 1.43, and 1.48) and a glucose unit (δ_{H} 3.99, 4.02, 4.23, 4.27, 4.42, 4.61, and 4.99). The ^{13}C NMR data, HSQC, and DEPT (135°) spectra of **3** exhibited 26 carbon resonances, including three methyls, eight methylenes, ten methines, and five sp^3 carbons. The COSY and HSQC spectra established four fragments: $\text{CH}-\text{CH}_2-\text{CH}$, CH_2-CH_2 , $\text{CH}-\text{CH}-\text{CH}_2-\text{CH}-\text{CH}_2$, and $\text{CH}-\text{CH}(\text{OH})-\text{CH}(\text{OH})-\text{CH}(\text{OH})-\text{CH}-\text{CH}_2(\text{OH})$. These structural features are consistent with a grayanane-type diterpenoid glycoside. The overall structural connectivity was established by HSQC and HMBC spectroscopic data. The HMBC correlations from H₂-20 (δ_{H} 5.05 and 5.47) to C-1 (δ_{C} 48.7)/C-9 (δ_{C} 54.5)/C-10 (δ_{C} 149.7) established an exocyclic $\Delta^{10(20)}$ double bond. The HMBC correlations from H₃-18/H₃-19/H₂-2 to C-3 (δ_{C} 90.1), from H-1/H₂-6/H₂-7/H₃-18/H₃-19 to C-5 (δ_{C} 83.7), from H-9/H₂-12/H-13 to C-11 (δ_{C} 84.5), and from



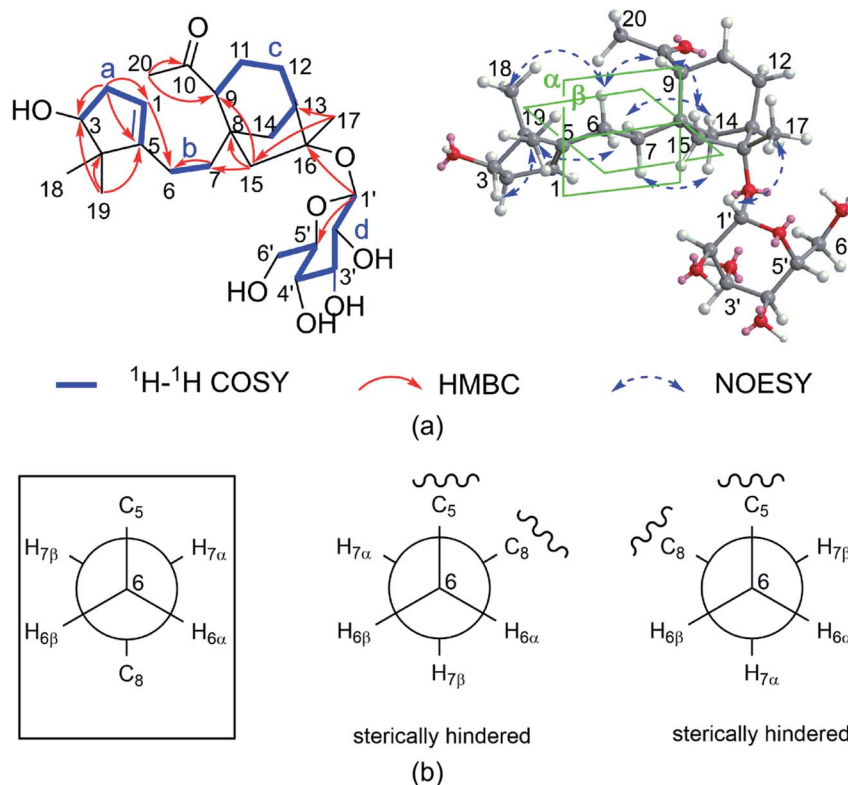


Fig. 2 (a) Key ^1H - ^1H COSY, HMBC, and NOESY correlations for **1**. (b) Conformations of C-6 and C-7, boxes indicate conformations that agree with the measured data and are energetically favored.

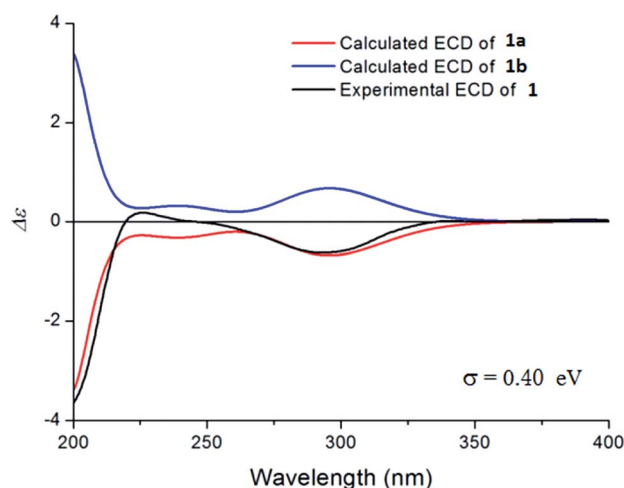


Fig. 3 The experimental CD spectrum of **1** (black) and the calculated ECD spectra of **1a** (red) and its enantiomer **1b** (blue).

$\text{H}_3\text{-17}/\text{H}_2\text{-14}/\text{H}_2\text{-12}/\text{H}_2\text{-13}$ to C-16 (δ_{C} 77.4) indicated the location of four oxygenated sp^3 carbons (C-3, C-5, C-11, and C-16). The skeleton (five rings including sugar part) and the exocyclic double bond accounted for six of the IHDs. The HMBC correlation from H-11 to C-16 suggested that C-11 and C-16 were connected *via* oxygen bridge. The glucose unit was placed at C-3 based on the HMBC correlation from H-1' to C-3. The anomeric

proton at H-1' (δ_{H} 4.99) showed a large coupling constant (7.8 Hz), indicating that the glucose unit is found in the β -configuration. Acid hydrolysis and GC analysis of the sugar moiety of **3** confirmed that the sugar was D -glucose (retention time: 29.56 min). The relative configuration of **3** was determined by the NOESY spectrum. The correlations of H-1/ $\text{H}_3\text{-18}$, H-3/ $\text{H}_3\text{-18}$, and H-1/ $\text{H}_6\alpha$ indicated that H-1 and H-3 are cofacial (α -face) and HO-5 should be β -oriented. The correlations of H-9/ $\text{H}_2\text{-15}$ and $\text{H}_3\text{-17}/\text{H}_2\text{-12}\beta$ indicated that H-9 and $\text{CH}_3\text{-17}$ are cofacial (β -face). Thus, the structure of **3** was defined as $11\beta,16\alpha$ -epoxy-3 β -[$(\beta\text{-D}$ -glucopyranosyl)oxy]-5 β -hydroxygrayanan-10(20)-ene.

Compound **4** (micranthanoside IV) was obtained as white powder. Its molecular formula was defined as $\text{C}_{26}\text{H}_{38}\text{O}_7$ based on HRESIMS (m/z 485.2492 [$\text{M} + \text{Na}$] $^+$, calcd 485.2510), which indicated an IHD of eight. Preliminary ^1H and ^{13}C analyses of **4** indicated the presence of a common grayanane skeleton. The NMR spectroscopic data of **4** were comparable to those of pierisformoside C.¹⁶ The only difference was the location of the double bond. The HMBC correlations from $\text{H}_3\text{-20}/\text{H}_2\text{-11}$ to C-9 (δ_{C} 142.6)/C-10 (δ_{C} 124.3) located the double bond at $\Delta^{9,10}$ instead of $\Delta^{10,20}$. The glucose unit was placed at C-3 based on the HMBC correlation from H-1' to C-3. The anomeric proton at H-1' (δ_{H} 5.03) showed a large coupling constant (7.8 Hz), indicating that the glucose unit is in β -configuration. Acid hydrolysis gave a D -glucose, which was identified by GC analysis (retention time: 29.49 min). In the NOESY spectrum, the correlations of H-3/ $\text{H}_3\text{-18}$ indicated that H-3 is α -oriented. Thus,



Table 2 ¹H NMR spectroscopic data for compounds 8–11 in pyridine-*d*₅ (δ in ppm, *J* in Hz)

No	8 ^b	9 ^a	10 ^a	11 ^a
1	2.78, dd (11.9, 7.4)	3.14, m	3.26, t (9.3)	3.18, t (9.4)
2	1.54, m	2.13, m	2.16, dd (14.0, 9.3)	2.23, m
	1.65, m	2.67, m	2.31, m	2.64, m
3	1.47, m	4.01, m	4.11, brs	3.94, d (5.0)
	2.39, m	—	—	—
4	—	—	—	—
5	—	—	—	—
6	1.66, m	1.67, m	1.38, m	4.48, d (8.6)
	1.72, m	1.67, m	1.53, m	—
7	1.83, m	1.68, m	1.72, m	2.02, d (13.7)
	1.89, m	1.73, m	2.67, m	2.76, dd (14.4, 9.8)
8	—	—	—	—
9	2.13, m	3.11, m	2.29, m	2.80, m
10	—	—	—	—
11	1.77, m	1.80, m	1.63, m	1.57, m
	1.77, m	1.80, m	1.82, m	1.72, m
12	1.60, m	1.63, m	1.59, m	1.39, m
	2.14, m	2.35, m	1.81, m	1.73, m
13	2.44, m	2.51, brs	2.62, m	2.22, brs
14	1.64, m	1.50, m	1.88, d (11.1)	1.92, d (11.1)
	2.20, m	1.70, m	2.22, m	2.36, dd (11.0, 4.1)
15	1.79, d (13.4)	1.88, d (14.0)	1.69, d (13.9)	2.11, d (13.7)
	2.33, d (14.1)	2.33, d (14.3)	2.26, d (15.0)	2.29, d (14.0)
16	—	—	—	—
17	1.62, s	1.62, s	1.60, s	1.55, s
18	3.83, m	0.80, s	0.80, s	1.34, s
	3.99, m	—	—	—
19	1.05, s	1.29, s	1.28, s	1.69, s
20	5.22, s	5.10, s	5.17, s	5.19, s
	5.31, s	5.14, s	5.19, s	5.22, s
1'	4.99, m	5.00, d (7.8)	5.00, (8.5)	4.98, d (7.7)
2'	3.97, m	4.01, m	3.99, brs	4.02, t (8.1)
3'	4.27, m	4.28, m	4.27, m	4.17, m
4'	4.25, m	4.27, m	4.27, m	4.18, m
5'	3.91, m	3.93, brs	3.93, brs	3.87, brs
6'	4.36, m	4.39, dd (11.6, 5.0)	4.40, m	4.34, dd (11.4, 5.4)
	4.50, d (11.5)	4.52, dd (11.5, 2.2)	4.54, d (11.3)	4.54, dd (11.4, 2.7)

^a Recorded at 500 MHz. ^b Recorded at 600 MHz.

the structure of **4** was defined as 3β-[(β-D-glucopyranosyl)oxy]-16α-hydroxygrayanan-1(5),6(7),9(10)-triene.

HRESIMS analysis of compound **5** (micranthanoside V) indicated a molecular formula of C₂₆H₄₂O₉. Spectroscopic data for **5** resembled those of pioside C, which differs from **5** with regard to the position of the glucose unit.¹⁷ The HMBC correlations from H-1' to C-16 placed the glucose unit at C-16 instead of C-3 as in pioside C. A large coupling constant (7.8 Hz) of the anomeric proton indicated the β-configuration of the glucose. In the NOESY spectrum, the correlations of H₃-18/H-1, H₃-18/H-3, and H₃-18/H-6 indicated that H-1, H-3, and H-6 are α-oriented, and the correlations of H₃-17/H-11β indicated that CH₃-17 is β-oriented. Acid hydrolysis and GC analysis of the sugar moiety of **5** confirmed that the sugar was D-glucose (retention time: 29.60 min). Thus, the structure of **5** was defined as 16α-[(β-D-glucopyranosyl)oxy]-3β,5β,6β-trihydroxygrayanan-9(10)-ene.

Compound **6** (micranthanoside VI) was found by mass spectrometry to have a molecular formula of C₂₆H₄₀O₇. The ¹H

and ¹³C NMR spectroscopic data indicated that **6** has a grayanane skeleton. Its ¹³C NMR spectrum exhibited the typical resonances of two double bonds and an anomeric carbon at δ_C 107.2, 152.4, 118.3, 156.4, and 99.8. Further HSQC and HMBC experiments allowed full assignment of the ¹H and ¹³C NMR spectra of **6**. The location of the two double bonds (Δ^{5,6}, Δ^{10,20}) was determined *via* HMBC correlations from H-1 to C-5/C-10, from H₂-20 to C-1/C-9/C-10, and from H₂-7 to C-5/C-6. The glucose unit was placed at C-16, which was supported by the HMBC correlation from H-1' to C-16. Acid hydrolysis and GC analysis of the sugar moiety of **6** confirmed that the sugar was D-glucose (retention time: 29.56 min). The relative configuration of **6** was established by the NOESY experiment. The correlations of H-1/H₃-18, H₃-18/H-3, and H-1/H-9 indicated that H-1, H-3, and H-9 are α-oriented. Thus, the structure of **6** was defined as 9-*epi*-16α-[(β-D-glucopyranosyl)oxy]-3β-hydroxygrayanan-5(6),10(20)-diene.

Compound **7** (micranthanoside VII) was determined to have the formula C₂₆H₄₀O₇. The planar structure of **7** was found to be



Table 3 ^1H NMR spectroscopic data for compounds **12**–**15** in pyridine- d_5 (δ in ppm, J in Hz)

No	12 ^a	13 ^a	14 ^a	15 ^a
1	1.72, m 1.97, m	1.46, m 2.07, m	1.46, m 1.96, m	1.66, t (13.7)
2	1.42, m 1.72, m	1.84, dd (13.9, 2.4) 2.14, m	1.43, m 1.82, m	2.18, m 2.56, m
3	4.68, dd (11.4, 1.9) —	3.65, d (2.5) —	0.92, d (12.7) 2.68, td (13.3, 4.1)	3.99, m —
4	—	—	—	—
5	—	—	—	—
6	4.09, brs —	—	—	2.53, m —
7	2.07, m 2.45, t (12.1)	2.22, d (11.6) 3.96, d (11.4)	2.21, d (11.8) 4.07, d (11.9)	1.78, m 1.78, m
8	—	—	—	—
9	2.09, m	2.59, d (8.7)	2.57, d (8.5)	1.95, m
10	—	—	—	—
11	1.42, m 1.60, d (13.1)	1.46, m 1.64, m	1.57, m 1.62, m	1.59, m 1.94, m
12	1.51, m 1.60, m	1.53, m 1.57, m	1.48, m 1.56, m	1.52, m 1.59, m
13	2.54, brs	2.51, brs	2.52, brs	2.12, d (2.9)
14	1.96, m 2.29, m	1.92, d (11.4) 2.30, dd (11.3, 4.0)	1.91, d (11.4) 2.28, m	1.78, t (12.8) 2.02, m
15	1.60, d (13.1) 2.39, d (14.0)	1.74, d (14.1) 2.35, d (14.1)	1.75, d (14.1) 2.31, d (14.3)	1.86, d (13.9) 2.04, m
16	—	—	—	—
17	1.66, s	1.62, s	1.61, s	1.54, s
18	4.83, s 5.10, s	1.52, s	1.31, s	1.20, s
19	1.74, s	1.50, s	3.4, d (8.3) 4.56, dd (10.7, 4.7)	1.51, s
20	1.23, s —	1.12, s —	1.11, s —	4.89, s 5.06, s
1'	4.99, d (7.8)	4.96, d (7.8)	4.95, d (8.1)	5.02, d (7.7)
2'	3.98, brs	3.97, m	3.96, brs	4.08, t (8.2)
3'	4.29, m	4.25, m	4.25, m	4.31, m
4'	4.29, m	4.27, m	4.27, m	4.28, m
5'	3.93, brs	3.91, brs	3.91, brs	4.02, m
6'	4.40, m 4.52, d (10.1)	4.38, dd (11.6, 5.1) 4.51, dd (11.6, 2.3)	4.39, d (12.4) 4.51, d (11.4)	4.41, dd (11.6, 5.4) 4.59, dd (11.6, 2.4)

^a Recorded at 500 MHz.

identical to that of **6** except for the location of the sugar moiety. The HMBC correlations from H-1' to C-3 placed the sugar moiety at C-3. The correlations of H₃-18/H-3, H-3/H-1, and H-1/H-9 in the NOESY spectrum indicated that H-1, H-3, and H-9 are α -oriented. Thus, the structure of **7** was defined as 9-*epi*-3- β -[[β -D-glucopyranosyl]oxy]-16 α -hydroxygrayanan-5(6),10(20)-diene.

The formula of compound **8** (micranthanoside VIII) was identified as C₂₆H₄₂O₈ by HRESIMS, indicating an IHD of six. The ^1H (Table 2) and ^{13}C NMR data of **8** were similar to those of micranthanoside E,¹³ except for the differences associated with the locations of the hydroxy groups. In micranthanoside E, the hydroxy groups were placed at C-3 and C-6. However, the hydroxy group was placed at C-18 in **8** indicated by the HMBC correlations from H₃-19/H₂-3 to C-18. The NOESY correlations of H-1/H₃-19, H-1/H-9, H-9/H-15 β , and H₃-17/H-12 β suggested that H-1, H-9, CH₃-17 and CH₃-19 are β -oriented. Thus, the

structure of **8** was defined as 1-*epi*-16 α -[[β -D-glucopyranosyl]oxy]-5 β -hydroxygrayanan-10(20)-ene-18-ol.

Compound **9** (micranthanoside IX) exhibited a molecular formula of C₂₆H₄₂O₈ based on the HRESIMS results. The ^1H and ^{13}C NMR spectroscopic data suggested that **9** has a grayanane skeleton similar to that of a known analogue, 6-deoxygrayanotoxin XVII,¹⁸ and an extra sugar moiety was the only difference. The glucose unit was placed at C-16 based on the HMBC correlation from H-1' to C-16. The NOESY correlations of H-1/H₃-18, H₃-17/H-12 β , and H-9/H₃-17 indicated that H-1 is α -oriented and H-9 and CH₃-17 are β -oriented. Acid hydrolysis and GC analysis of the sugar moiety of **9** confirmed that the sugar was D-glucose (retention time: 29.53 min). Thus, the structure of **9** was defined as 16 α -[[β -D-glucopyranosyl]oxy]-3 β ,5 β -dihydroxygrayanan-9(10)-ene.



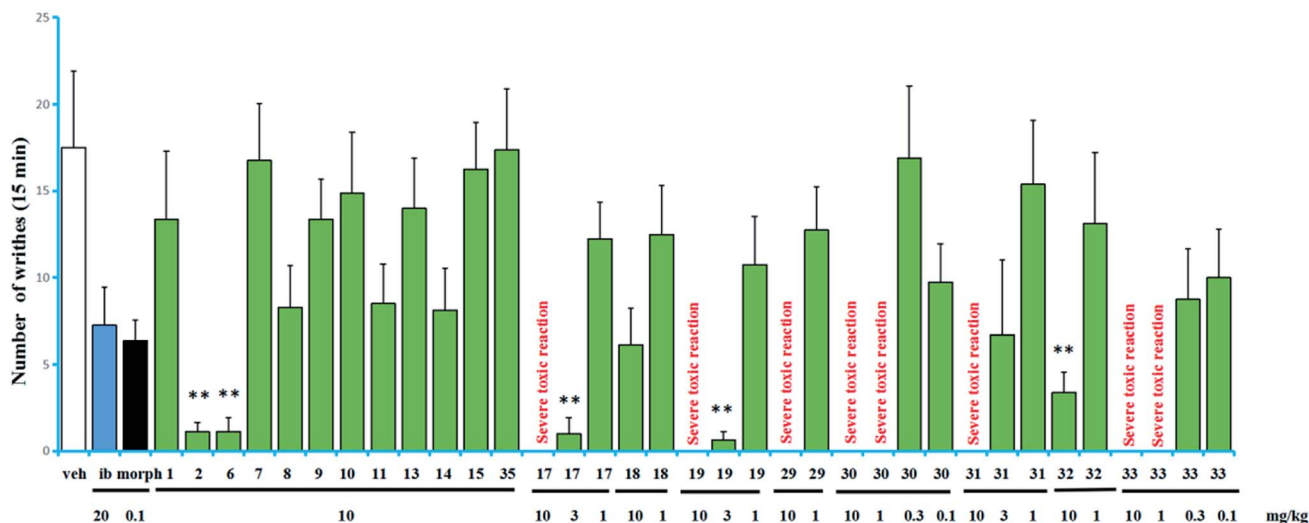


Fig. 4 Antinociceptive activities of partial diterpenoids isolated from *R. micranthum*. Data represent the mean \pm SEM. * $p < 0.05$, ** $p < 0.01$, vs. vehicle (veh). Control drugs: ibuprofen (ib) and morphine (morph).

The molecular formula of compound **10** (micranthanoside X) was determined as $C_{26}H_{42}O_8$, implying an IHD of six. The HSQC and HMBC spectra indicated that the planar structure of **10** was the same as that of **9**. The NOESY correlations of H-1/H-9, H-1/HO-5, H₃-19/HO-5, and H₃-17/H-12 β in **10** indicated that H-1 is β -oriented, which is the only difference between the two compounds. Acid hydrolysis and GC analysis of the sugar moiety of **10** confirmed that the sugar was D-glucose (retention time: 29.55 min). Thus, the structure of **10** was defined as 1-*epi*-16 α -[[β -D-glucopyranosyl]oxy]-3 β ,5 β -dihydroxygrayanan-9(10)-ene.

The molecular formula of compound **11** (micranthanoside XI) was determined as $C_{26}H_{42}O_9$, implying an IHD of six. The ¹H and ¹³C NMR data of **11** were similar to that of grayanotoxin-XVIII (**17**) except for signal of an additional sugar moiety.¹⁹ The glucose unit was placed at C-6 as suggested by the HMBC correlations from H-1' to C-6. The NOESY correlations of H-3/H₃-18, H-1/H-6, H-6/H₃-18, H-1/

H₃-18, H₃-17/H-9, and H-9/H-15 β indicated that H-1, H-3, and H-6 are α -oriented and H-9 and H₃-17 are β -oriented. Thus, the structure of **11** was defined as 6 β -[[β -D-glucopyranosyl]oxy]-3 β ,5 β ,16 α -trihydroxygrayanan-9(10)-ene.

Compound **12** was obtained as white powder and determined to have the molecular formula $C_{26}H_{42}O_9$ by HRESIMS. The ¹H (Table 3) and ¹³C NMR spectroscopic data suggested that **12** has a 4,5-*seco-ent*-kaurane skeleton similar to known analogues.¹⁴ The ¹H, ¹³C, and HSQC NMR data for **12** indicated the presence of a sugar unit (δ_C 63.4, 72.3, 75.8, 78.3, 79.4, and 99.9) and two olefinic carbons (δ_C 110.5 and 148.0). The overall structural connectivity was established by HSQC and HMBC spectroscopic data. The HMBC correlations from HO-5 to C-5/C-10 and from H-6 to C-7 placed two hydroxy groups at C-5 and C-6. The sugar unit was placed at C-16 as suggested by HMBC correlations of H-1' to C-16. An oxygen bridge should be present between C-3 and C-5, which was supported by the HMBC correlation from H-3 to C-5. The

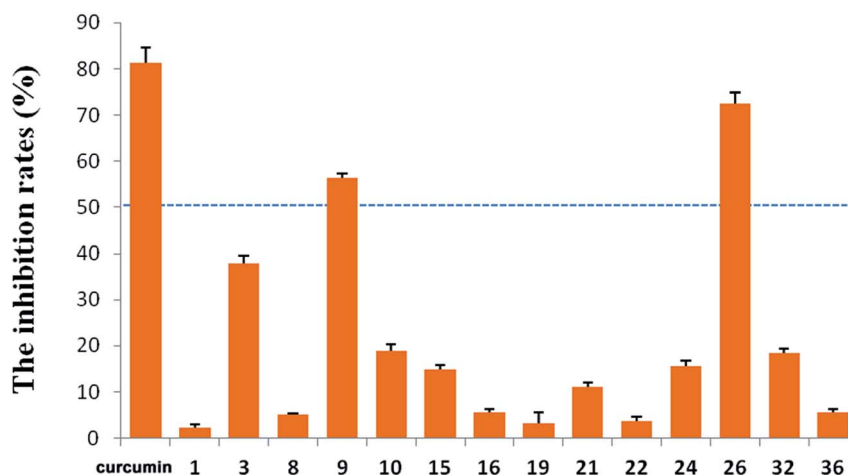


Fig. 5 Inhibitory effects of LPS-induced NO production in BV2 cells.



Table 4 ^{13}C NMR spectroscopic data for compounds 1–16 in pyridine- d_5 (δ in ppm)

No.	1 ^b	2 ^b	3 ^b	4 ^a	5 ^a	6 ^a	7 ^b	8 ^a	9 ^a	10 ^b	11 ^a	12 ^a	13 ^a	14 ^b	15 ^a
1	118.9	118.9	48.7	138.7	45.1	46.8	46.6	54.8	47.6	60.6	45.2	32.1	28.2	33.2	42.5
2	39.0	37.8	34.7	41.2	37.7	37.4	36.2	26.5	39.3	36.7	39.9	26.8	26.3	18.3	30.7
3	81.5	89.8	90.1	87.8	81.1	80.6	89.8	33.2	80.7	83.3	82.3	72.9	77.7	32.6	82.3
4	49.1	49.0	51.4	49.6	49.5	46.7	46.6	50.5	50.7	50.3	51.7	148.0	40.9	40.3	51.3
5	152.1	151.5	83.7	144.8	85.7	156.4	155.7	83.7	84.2	85.6	84.0	99.6	85.3	84.4	213.6
6	23.6	23.0	32.2	122.7	68.4	118.3	118.1	26.2	32.2	29.4	79.1	71.1	213.7	216.3	48.3
7	38.6	38.3	34.2	130.9	46.8	41.9	42.6	39.3	31.8	36.4	41.8	44.8	51.7	52.5	22.2
8	47.3	47.2	47.7	50.0	51.1	46.6	46.7	47.7	46.7	47.2	45.1	45.5	50.0	49.8	46.4
9	53.6	54.2	54.5	142.6	136.3	55.8	55.7	54.6	47.5	55.9	53.7	42.6	48.5	47.4	49.9
10	212.9	213.0	149.7	124.3	122.1	152.4	151.9	151.0	154.4	155.3	153.0	40.9	48.7	48.5	151.8
11	22.9	22.7	84.5	24.1	27.3	26.6	26.3	25.5	25.3	28.1	26.0	18.8	18.5	18.4	36.6
12	25.7	26.0	39.8	26.4	29.3	25.5	25.8	33.4	37.8	27.0	24.4	27.2	27.0	27.2	25.3
13	46.7	49.3	45.6	46.4	45.8	47.8	50.2	47.0	46.7	47.1	48.4	46.8	46.9	46.8	50.4
14	37.9	37.8	44.1	39.8	48.8	35.6	36.0	36.6	24.9	35.6	36.8	38.8	38.7	38.8	39.9
15	51.2	53.3	57.9	52.5	55.9	55.4	58.2	56.2	57.8	55.5	63.6	56.3	56.6	56.9	55.9
16	88.1	79.2	86.7	80.6	90.1	88.5	79.6	88.9	89.2	88.2	80.0	86.9	86.9	86.9	79.0
17	21.4	25.2	24.0	29.5	21.7	21.1	24.8	21.5	21.8	21.6	26.3	21.8	21.6	21.6	25.0
18	25.8	25.9	25.6	26.5	24.8	28.1	28.3	68.0	24.3	23.7	23.9	110.5	25.1	20.6	20.6
19	20.3	20.5	18.8	21.7	18.3	24.2	24.5	23.5	17.9	19.3	19.9	19.1	24.4	72.0	22.7
20	32.6	32.7	114.6	18.2	20.6	107.2	107.5	111.3	111.7	109.8	112.9	23.5	20.9	20.2	106.5
1'	99.8	106.5	105.7	106.5	99.8	99.8	106.6	99.8	99.8	99.9	103.0	99.9	99.8	99.9	103.2
2'	75.8	76.0	76.1	76.0	75.8	75.9	76.0	75.7	75.9	75.8	75.5	75.8	75.8	75.8	75.7
3'	79.3	79.1	79.2	79.2	79.3	79.4	79.2	79.4	79.4	79.3	79.0	79.4	79.3	79.3	79.2
4'	72.3	72.2	72.2	72.3	72.3	72.4	72.3	72.3	72.4	72.3	72.6	72.3	72.2	72.2	72.4
5'	78.6	78.9	79.1	78.9	78.5	78.7	78.9	78.6	78.6	78.6	78.7	78.7	78.6	78.6	79.0
6'	63.5	63.4	63.4	63.5	63.4	63.4	63.4	63.5	63.5	63.5	63.6	63.4	63.4	63.4	63.5

^a Recorded at 125 MHz. ^b Recorded at 150 MHz.

NOESY correlations of H-3/H-1 β , H-1 β /H-9, H-9/H-12 β , and H₃-20/H-6 suggested that H-3 and H-9 are β -oriented and H-6 is α -oriented. Thus, the structure of **12** was named as micranthanoside XII. Micranthanoside XII (**12**) represent the first example of 3,5-epoxy-4,5-seco-*ent*-kaurane diterpenoid.

Compound **13** (micranthanoside XIII) has a molecular formula of C₂₆H₄₂O₉. Preliminary analyses of the NMR data indicated the presence of an *ent*-kaurane skeleton. The NMR spectra indicated the presence of two hydroxy groups, a carbonyl group, and a sugar moiety. The two hydroxy groups were placed at C-3 and C-5 on the basis of the correlations from HO-3 to C-2/C-3/C-4 and from HO-5 to C-4/C-5/C-6, respectively. The HMBC correlation from H-1' to C-16 indicated that the sugar moiety was located at C-16. The HMBC correlations from H₂-7 to C-6 placed the carbonyl group at C-6. In the NOESY spectrum of **13**, correlations of H-3/HO-5, H-3/H₃-19, H₃-18/HO-3, H₃-20/H-14 α , and H-9/H-15 β indicated that H-3, HO-5, and H-9 are β -oriented and CH₃-20 is α -oriented. Acid hydrolysis and GC analysis of **13** confirmed that the sugar moiety was D-glucose (retention time: 29.54 min). Thus, the structure of **13** was defined as 16 α -[(β -D-glucopyranosyl)oxy]-3 α ,5 β -dihydroxy-*ent*-kaur-6-one.

Compound **14** (micranthanoside XIV) has a molecular formula of C₂₆H₄₂O₉. The ¹H and ¹³C NMR data of **14** were similar to those of **13**. The HMBC correlations from H₃-18 to C-19 indicated that the hydroxy group was at C-19 in **14** instead of at C-3 as in **13**. In the NOESY spectrum, the correlations of H₃-20/H₃-18, H₃-20/H-14 α , and H-9/H-15 β

indicated that H-9 is β -oriented and CH₃-20 is α -oriented. Acid hydrolysis and GC analysis of **14** confirmed that the sugar moiety was D-glucose (retention time: 29.50 min). Thus, the structure of **14** was defined as 16 α -[(β -D-glucopyranosyl)oxy]-5 β -hydroxy-*ent*-kaur-6-one-19-ol.

Compound **15** (micranthanoside XV) has a molecular formula of C₂₆H₄₀O₈. Preliminary ¹H and ¹³C analyses of **15** indicated the presence of a leucothane skeleton. The ¹³C NMR spectrum displayed resonances of a carbonyl group, a sugar moiety and a double bond. The sugar moiety and the carbonyl group were placed at C-3 and C-5 based on the HMBC correlations from H-1' to C-3 and from H₃-18/H₃-19/H-6 to C-5, respectively. The HMBC correlations from H₂-20 to C-1/C-9/C-10 suggested that the exocyclic double bond is $\Delta^{10(20)}$. The NOESY correlations of H-3/H-1, H-3/H₃-19, H-6/H₃-18, and H-9/H-15 β indicated that H-1, H-3, and H-9 are β -oriented and H-6 is α -oriented. Acid hydrolysis and GC analysis confirmed that the sugar moiety was D-glucose (retention time: 29.64 min). Thus, the structure of **15** was defined as 3 α -[(β -D-glucopyranosyl)oxy]-16 α -hydroxyleucoth-10(20)-en-5-one.

The known compounds micranthanoside F (**16**),¹³ grayanotoxin XVIII (**17**),¹⁹ pierisformosin A (**18**),²⁰ 6-deoxy-1-*epi*-grayanotoxin XVII (**19**),¹⁸ grayanotoxin IV (**20**),²¹ grayanoside C (**21**),²² grayanotoxin II (**22**),²³ grayanoside B (**23**),¹⁹ micranthanosides C (**24**) and A (**25**),¹³ rhodomicanoside F (**26**),¹⁴ grayanotoxins I (**27**),²¹ III (**28**),²⁴ VII (**29**),²⁵ IX (**30**),²⁶ and VIII (**31**),²⁶ 19-sophorosyl kaurenoate (**32**),²⁷ kalmanol (**33**),²⁸



rhodomicrosides A (34),¹⁴ picroside B (35),²⁹ and picrosides F (36)¹⁶ were determined by comparison of their experimental NMR data with those reported in the literature.

The acetic acid-induced writhing test is usually used as a sensitive model for measuring acute pain.^{6–9} Compounds 1–2, 6–11, 13–15, 17–19, 29–33, and 35 were evaluated in the test for their antinociceptive activity based on the inhibition rates of writhes. In this test, intraperitoneal (IP) administration was used for all of the compounds. The obtained data are summarized in Fig. 4. Compounds 17 and 19 showed higher inhibitory activities than the other tested compounds, inhibited 94.3% and 96.4% of the writhes, respectively, when administered at a dose of 3 mg kg⁻¹. However, they showed severe toxic reactions when administered at a dose of 10 mg kg⁻¹. Compounds 2, 6 and 32 showed significant antinociceptive activity at a dose of 10 mg kg⁻¹. In contrast, in the same assay, ibuprofen inhibited 58.6% of the writhes when administered at a dose of 20 mg kg⁻¹ while morphine inhibited 63.6% of the writhes when administered at a dose of 0.1 mg kg⁻¹.

Compounds 17, 19, 29–31, (grayananes) and 33 (kalmene) produced antinociceptive effects at lower doses while showed toxic reactions at higher doses. Mice given higher doses showed reactions of nausea and convulsion, which is consistent with the clinical symptoms of “zhaoshanbai” poisoning.^{5–7} The results in this test and those reported previously revealed that among the antinociceptive components, grayananes and kalmene are responsible for both antinociceptive and toxic effects. Their antinociceptive activity was positively correlated with the toxicity.^{8,13,30} Some kauranes and leucothanes also showed significant antinociceptive activity at relatively high doses, but no toxic reaction was observed.^{10,14} This fact suggests that they may have different mechanisms of action.

The preliminary analysis of the structures (present and reported) and their bioactivities revealed that the presence of sugar unit at C-3, C-6, or C-16 decreases the activity as well as the toxicity (as in 11/17, 10/19, 15/rhodomicrosin I, rhodomicrosides E/rhodomicrosone E).^{10,14} Compound 2 is more active than 1, which suggested that sugar unit at C-3 is likely to hinder activity to a lesser degree. Traditionally, “zhaoshanbai” was extracted by water decoction. Diterpenoid glycosides rather than the aglycones were the main components of the extract because of the polarity, which reduced the toxicity of the extract to a certain extent.^{31,32} However, in order to ensure clinical safety, the content of diterpenoid aglycones in extracts still needs to be monitored.

R. micranthum (zhaoshanbai) has also been widely used as an anti-inflammatory drug to alleviate the symptoms of upper respiratory inflammation. Therefore, the anti-inflammatory activities of the compounds 1–3, 7–11, 13–32, and 34–36 were evaluated by measuring inhibitory effects of LPS-induced NO production in BV2 cells. At 10 μM, compounds 9 and 26 displayed moderate activity with inhibition rates of 56.31% and 72.43%, respectively (Fig. 5). At the same concentration, the inhibition rate of the positive control (curcumin) is 81.38%.

Conclusion

A total of 36 diterpenoids, including fifteen new diterpenoid glycosides (1–15) and 21 known analogues were obtained from the leaves and twigs of *R. micranthum*. In the acetic acid-induced writhing test, compounds 17 and 19 showed significant antinociceptive activity at a dose of 3 mg kg⁻¹ and compounds 2, 6 and 32 showed significant antinociceptive activity at a dose of 10 mg kg⁻¹. Grayananes and kalmene such as 17, 19, 29–31, 33 are both antinociceptive and toxic components. In addition, micranthoside IX (9) and rhodomicrosides F (26) showed moderate anti-inflammatory activity by reducing LPS-induced NO production in BV2 cells.

Experimental section

General experimental procedures

IR spectra were recorded using a Nicolet 5700 FT-IR spectrometer. Optical rotations were acquired *via* a Rudolph automatic polarimeter. HRESIMS analysis was carried out using an Agilent 6520 Accurate-Mass Q-TOF LC/MS spectrometer. NMR spectra were obtained using INOVA-500, Bruker AV600-III and INOVA SX-600 spectrometers. A Shimadzu LC-6AD instrument (SPD-20A and RID-10A detectors) was used for preparative HPLC separations. Liquid chromatography was conducted using a YMC ODS column. A D101-type macroporous resin, Baoen Corporation (Cangzhou, China); Sephadex LH-20, GE Chemical Corporation (USA); silica gel and GF254 TLC plates, Jiangyou Corporation (Yantai, China); and ODS (50 μm), Merck (Germany) were used for column chromatography (CC). TLC analyses were carried out on precoated silica gel GF254 plates, and spots were visualized under UV light (254 and 365 nm) or by heating after spraying with a 5% CH₃CH₂OH–H₂SO₄ solution.

Plant material

Twigs and leaves of *R. micranthum* were collected from Yiyuan, Shandong Province in August 2014. The plant was authenticated by Prof. Peng Wan (Shandong University of Traditional Chinese Medicine). A voucher specimen (ID-s-2586) was deposited in the herbarium of Institute of Materia Medica, Chinese Academy of Medical Sciences.

Extraction and isolation

Twigs and leaves of *R. micranthum* (107.5 kg) were air-dried and extracted twice (2 h each time) with EtOH under reflux. The ethanol extracts were evaporated under reduced pressure, and the residue was suspended in water and then partitioned successively with petroleum ether, CH₂Cl₂, EtOAc, and *n*-BuOH. The EtOAc extract was separated using a macroporous resin column eluted sequentially with 70 : 30, 40 : 60, and 5 : 95 (v/v) H₂O–EtOH solutions. Then, silica gel CC was used to separate the 60% EtOH fraction (288.4 g). The column was eluted with a step gradient of CH₂Cl₂/MeOH (20 : 1, 10 : 1, 5 : 1, and 1 : 1, v/v). Fractions E₆₀G₁–E₆₀G₉ were collected based on the TLC results. Fraction E₆₀G₂ was purified *via* semipreparative HPLC (MeCN–H₂O, 37 : 63, v/v, 3.5 ml min⁻¹) to afford 30 (5.5 mg, *t*_R =



37.5 min). Fraction E₆₀G₃ was separated *via* a Sephadex LH-20 column eluted with MeOH–H₂O (60 : 40, v/v) and yielded three fractions (E₆₀G₃L₁–E₆₀G₃L₃). E₆₀G₃L₂ was purified *via* semipreparative HPLC (MeCN–H₂O, 25 : 75, v/v, 3.5 ml min⁻¹) to afford **17** (72.4 mg, *t*_R = 35.4 min), **29** (20.8 mg, *t*_R = 38.6 min), **31** (5.5 mg, *t*_R = 40.9 min), **28** (2.1 mg, *t*_R = 15.7 min), **18** (9.9 mg, *t*_R = 45.6 min), **27** (52.3 mg, *t*_R = 50.3 min). Fraction E₆₀G₆ was further separated using a Sephadex LH-20 column eluted with MeOH–H₂O (60 : 40, v/v) and yielded 2 fractions (E₆₀G₆L₁–E₆₀G₆L₂). Fraction E₆₀G₆L₁ (20.0 g) was separated using an MCI column and eluted with a step gradient of MeOH/H₂O (40 : 60, 50 : 50, 60 : 40, 70 : 30, 80 : 20, and 100 : 0, v/v) to yield 6 fractions, E₆₀G₆L₁M₁ to E₆₀G₆L₁M₆. Fraction E₆₀G₆L₁M₂ was then separated *via* preparative HPLC (MeOH–H₂O, 50 : 50, v/v, 5 ml min⁻¹) and yielded nine fractions, E₆₀G₆L₁M₂-1 to E₆₀G₆L₁M₂-9. Fraction M₂-5 was purified *via* semipreparative HPLC (MeCN–H₂O, 17 : 83, v/v, 3.5 ml min⁻¹) to afford **24** (17.5 mg, *t*_R = 22.2 min), **25** (23.2 mg, *t*_R = 24.7 min), and **26** (8.7 mg, *t*_R = 28.7 min). Fraction M₂-6 was purified *via* semipreparative HPLC (MeCN–H₂O, 18 : 82, v/v, 3.5 ml min⁻¹) to afford **16** (6.0 mg, *t*_R = 22.7 min). Fraction M₂-7 was purified *via* semipreparative HPLC (MeCN–H₂O, 16 : 84, v/v, 3.5 ml min⁻¹) to afford **34** (12.0 mg, *t*_R = 36.9 min). Fraction M₂-8 was purified *via* semipreparative HPLC (MeCN–H₂O, 25 : 75, v/v, 3.5 ml min⁻¹) to afford **9** (23.1 mg, *t*_R = 15.1 min). Fraction M₂-9 was purified *via* semipreparative HPLC (MeCN–H₂O, 20 : 80, v/v, 3.5 ml min⁻¹) to afford **5** (1.8 mg, *t*_R = 20.4 min). Fraction E₆₀G₆L₁M₃ was then separated *via* preparative HPLC (MeOH–H₂O, 60 : 40, v/v, 5 ml min⁻¹) and yielded eleven fractions, E₆₀G₆L₁M₃-1 to E₆₀G₆L₁M₃-11. Fraction M₃-5 was purified *via* semipreparative HPLC (MeCN–H₂O, 25 : 75, v/v, 3.5 ml min⁻¹) to afford **19** (7.0 mg, *t*_R = 25.1 min) and **13** (122.4 mg, *t*_R = 28.7 min). Fraction M₃-6 was purified *via* semipreparative HPLC (MeCN–H₂O, 24 : 76, v/v, 3.5 ml min⁻¹) to afford **10** (27.3 mg, *t*_R = 29.4 min), **6** (40.1 mg, *t*_R = 29.4 min), and **7** (45.2 mg, *t*_R = 29.4 min). Fraction M₃-8 was purified *via* semipreparative HPLC (MeCN–H₂O, 27 : 73, v/v, 3.5 ml min⁻¹) to afford **3** (2.2 mg, *t*_R = 29.4 min). Fraction M₃-9 was purified *via* semipreparative HPLC (MeCN–H₂O, 30 : 70, v/v, 3.5 ml min⁻¹) to afford **4** (1.0 mg, *t*_R = 25.4 min). Fraction M₃-10 was purified *via* semipreparative HPLC (MeCN–H₂O, 30 : 70, v/v, 3.5 ml min⁻¹) to afford **8** (5.7 mg, *t*_R = 29.1 min) and **14** (12.6 mg, *t*_R = 40.8 min). Fraction M₃-11 afforded **12** (19.5 mg, *t*_R = 58.0 min) without purification. Fraction E₆₀G₈ was further separated *via* a Sephadex LH-20 column eluted with MeOH–H₂O (60 : 40, v/v) and yielded four fractions (E₆₀G₈L₁–E₆₀G₈L₄). Fraction E₆₀G₈L₃ afforded **32** (30.3 mg). Fraction E₆₀G₈L₂ was separated *via* preparative HPLC (MeOH–H₂O, 50 : 50, v/v, 5 ml min⁻¹) and yielded five fractions, E₆₀G₈L₂-1 to E₆₀G₈L₂-5. Fraction E₆₀G₈L₂-1 afforded **23** (106.6 mg). Fraction E₆₀G₈L₂-3 was purified *via* semipreparative HPLC (MeCN–H₂O, 20 : 80, v/v, 3.5 ml min⁻¹) to afford **21** (9.6 mg, *t*_R = 41.2 min). Fraction E₆₀G₈L₂-4 was purified *via* semipreparative HPLC (MeCN–H₂O, 20 : 80, v/v, 3.5 ml min⁻¹) to afford **11** (9.8 mg, *t*_R = 35.2 min).

The 30% EtOH fraction of the macroporous resin column was also loaded on a silica gel column and eluted with a step gradient of CH₂Cl₂/MeOH (20 : 1, 10 : 1, 5 : 1, and 1 : 1, v/v).

Fractions G₁–G₉ were collected based on the results of TLC analysis. Fraction E₃₀G₅ was further purified *via* a Sephadex LH-20 column to yield 2 fractions, E₃₀G₅L₁ and E₃₀G₅L₂. Fraction E₃₀G₅L₁ (37.7 g) was separated *via* an MCI column and eluted with a step gradient of MeOH/H₂O (10 : 90, 30 : 70, 40 : 60, 50 : 50, 60 : 40, 70 : 30, and 100 : 0, v/v) to yield 5 fractions, E₃₀G₅L₁M₁ to E₃₀G₅L₁M₅. Fraction E₃₀G₅L₁M₃ was separated *via* ODS column and eluted with a step gradient of MeOH/H₂O (40 : 60, 50 : 50, 70 : 30, 80 : 20 and 100 : 0, v/v) to yield 5 fractions, E₃₀G₅L₁M₃O₁ to E₃₀G₅L₁M₃O₅. Fraction E₃₀G₅L₁M₃O₄ was purified *via* preparative HPLC to afford eight fractions, E₃₀G₅L₁M₃O₄-1 to E₃₀G₅L₁M₃O₄-5. O₄-1 was purified *via* HPLC (MeCN–H₂O, 20 : 80, v/v) to afford **35** (2.1 mg, *t*_R = 48.7 min). O₄-2 was purified *via* HPLC (MeCN–H₂O, 25 : 75, v/v) to afford **1** (8.4 mg, *t*_R = 25.2 min) and **2** (4.9 mg, *t*_R = 32.9 min). Then, E₃₀G₅L₁M₄ was purified *via* preparative HPLC (MeCN–H₂O, 20 : 80, v/v) to afford eight fractions, E₃₀G₅L₁M₄-1 to E₃₀G₅L₁M₄-8. M₄-3 afforded **20** (13.5 mg, *t*_R = 15.5 min). M₄-4 was purified *via* HPLC (MeCN–H₂O, 25 : 75, v/v) to afford **15** (7.7 mg, *t*_R = 23.0 min). M₄-5 was purified *via* HPLC (MeCN–H₂O, 25 : 75, v/v) to afford **22** (8.9 mg, *t*_R = 16.6 min). M₄-8 was purified *via* HPLC (MeCN–H₂O, 30 : 70, v/v) to afford **36** (49.7 mg, *t*_R = 34.6 min). Fraction E₃₀G₅L₁M₅ was purified *via* HPLC (MeCN–H₂O, 13 : 87, v/v) to afford **33** (6.1 mg, *t*_R = 32.1 min).

Micranthanoside I (1). White powder; [α]_D²⁰ –49.1 (*c* 0.53, MeOH); IR ν_{\max} 3368, 2928, 1700, 1460, 1357, 1257, 1159, 1075, 1041, 883, 857, 812, 634 cm⁻¹; ¹H and ¹³C NMR data, see Tables 1 and 4; HRESIMS *m/z* 505.2786 [M + Na]⁺ (calcd for C₂₆H₄₂NaO₈, 505.2772).

Micranthanoside II (2). White powder; [α]_D²⁰ –83.3 (*c* 0.48, MeOH); IR ν_{\max} 3350, 2928, 1701, 1459, 1357, 1256, 1230, 1201, 1163, 1074, 911, 888, 811, 635 cm⁻¹; ¹H and ¹³C NMR data, see Tables 1 and 4; HRESIMS *m/z* 505.2781 [M + Na]⁺ (calcd for C₂₆H₄₂NaO₈, 505.2772).

Micranthanoside III (3). White powder; [α]_D²⁰ –58.1 (*c* 0.02, MeOH); IR ν_{\max} 3367, 2962, 1627, 1549, 1449, 1378, 1077, 947, 903, 830 cm⁻¹; ¹H and ¹³C NMR data, see Tables 1 and 4; HRESIMS *m/z* 503.2623 [M + Na]⁺ (calcd for C₂₆H₄₀NaO₈, 503.2615).

Micranthanoside IV (4). White powder; [α]_D²⁰ –50.0 (*c* 0.01, MeOH); IR ν_{\max} 3382, 2930, 2870, 1630, 1446, 1363, 1314, 1256, 1165, 1078, 1034, 929, 891, 759 cm⁻¹; ¹H and ¹³C NMR data, see Tables 1 and 4; HRESIMS *m/z* 485.2492 [M + Na]⁺ (calcd for C₂₆H₃₈NaO₇, 485.251).

Micranthanoside V (5). White powder; [α]_D²⁰ +9.0 (*c* 0.04, MeOH); IR ν_{\max} 3389, 2924, 1647, 1598, 1419, 1076, 911, 852, 805, 630 cm⁻¹; ¹H and ¹³C NMR data, see Tables 1 and 4; HRESIMS *m/z* 521.2722 [M + Na]⁺ (calcd for C₂₆H₄₂NaO₉, 521.2721).

Micranthanoside VI (6). White powder; [α]_D²⁰ –58.7 (*c* 0.06, MeOH); IR ν_{\max} 3380, 2937, 2869, 1633, 1548, 1447, 1046, 1379, 1307, 1266, 1156, 1073, 1034, 915, 890, 828 cm⁻¹; ¹H and ¹³C NMR data, see Tables 1 and 4; HRESIMS *m/z* 487.2676 [M + Na]⁺ (calcd for C₂₆H₄₀NaO₇, 487.2666).

Micranthanoside VII (7). White powder; [α]_D²⁰ –34.2 (*c* 0.06, MeOH); IR ν_{\max} 3379, 2937, 1728, 1677, 1549, 1375, 1306, 1243, 1201, 1080, 1048, 885, 643 cm⁻¹; ¹H and ¹³C NMR data, see



Tables 1 and 4; HRESIMS m/z 487.2671 $[M + Na]^+$ (calcd for $C_{26}H_{40}NaO_7$, 487.2666).

Micranthoside VIII (8). White powder; $[\alpha]_D^{20}$ -17.6 (c 0.06, MeOH); IR ν_{max} 3375, 2938, 2873, 1641, 1549, 1448, 1379, 1306, 1158, 1079, 1041, 940, 898, 858, 830, 769, 624, 536 cm^{-1} ; 1H and ^{13}C NMR data, see Tables 2 and 4; HRESIMS m/z 505.2788 $[M + Na]^+$ (calcd for $C_{26}H_{42}NaO_8$, 505.2772).

Micranthoside IX (9). White powder; $[\alpha]_D^{20}$ -48.6 (c 0.06, MeOH); IR ν_{max} 3407, 2937, 1628, 1448, 1382, 1264, 1158, 1077, 1041, 950, 898, 858, 639 cm^{-1} ; 1H and ^{13}C NMR data, see Tables 2 and 4; HRESIMS m/z 505.2775 $[M + Na]^+$ (calcd for $C_{26}H_{42}NaO_8$, 505.2772).

Micranthoside X (10). White powder; $[\alpha]_D^{20}$ -5.0 (c 0.03, MeOH); IR ν_{max} 3382, 2933, 1637, 1450, 1384, 1222, 1080, 1035, 916, 890, 859, 827, 647 cm^{-1} ; 1H and ^{13}C NMR data, see Tables 2 and 4; HRESIMS m/z 505.2766 $[M + Na]^+$ (calcd for $C_{26}H_{42}NaO_8$, 505.2772).

Micranthoside XI (11). White powder; $[\alpha]_D^{20}$ -27.8 (c 0.2, MeOH); IR ν_{max} 3368, 2927, 1701, 1460, 1357, 1163, 1074, 1031, 911, 888, 811, 635 cm^{-1} ; 1H and ^{13}C NMR data, see Tables 2 and 4; HRESIMS m/z 503.2612 $[M + Na]^+$ (calcd for $C_{26}H_{40}NaO_8$, 503.2615).

Micranthoside XII (12). White powder; $[\alpha]_D^{20}$ $+66.0$ (c 0.05, MeOH); IR ν_{max} 3393, 2926, 2850, 1645, 1596, 1468, 1453, 1417, 1384, 1261, 1157, 974, 633, 546 cm^{-1} ; 1H and ^{13}C NMR data, see Tables 3 and 4; HRESIMS m/z 521.2708 $[M + Na]^+$ (calcd for $C_{26}H_{42}NaO_9$, 521.2721).

Micranthoside XIII (13). White powder; $[\alpha]_D^{20}$ -92.0 (c 0.25, MeOH); IR ν_{max} 3557, 3526, 3481, 3330, 2942, 2885, 1716, 1659, 1461, 1434, 1386, 1102, 1076, 1042, 988, 943, 640, 601 cm^{-1} ; 1H and ^{13}C NMR data, see Tables 3 and 4; HRESIMS m/z 521.2719 $[M + Na]^+$ (calcd for $C_{26}H_{42}NaO_9$, 521.2721).

Micranthoside XIV (14). White powder; $[\alpha]_D^{20}$ -44.4 (c 0.08, MeOH); IR ν_{max} 3511, 3321, 2947, 2874, 1698, 1623, 1462, 1442, 1387, 1269, 1104, 1070, 1020, 997, 959, 855, 645, 574, 552 cm^{-1} ; 1H and ^{13}C NMR data, see Tables 3 and 4; HRESIMS m/z 521.2711 $[M + Na]^+$ (calcd for $C_{26}H_{42}NaO_9$, 521.2721).

Micranthoside XV (15). White powder; $[\alpha]_D^{20}$ -69.8 (c 0.07, MeOH); IR ν_{max} 3396, 2935, 2872, 1701, 1643, 1447, 1381, 1299, 1202, 1159, 1077, 1030, 991, 928, 886, 844, 595, 579 cm^{-1} ; 1H and ^{13}C NMR data, see Tables 3 and 4; HRESIMS m/z 503.2615 $[M + Na]^+$ (calcd for $C_{26}H_{40}NaO_8$, 503.2615).

Acid hydrolysis and GC analysis

The configuration of the sugar moiety was established according to a published method.³³ The compounds were dissolved in MeOH (2 ml) and then added to 2 N HCl (2 ml). The solution was heated at 90 °C for 12 h. The reaction mixture was evaporated and partitioned with EtOAc and H₂O. The aqueous layer was concentrated to dryness, dissolved in dry pyridine and reacted with L-cysteine methyl ester hydrochloride (2 mg) at 80 °C for 1 h. After removal of the solvent, *N*-trimethylsilylimidazole (1 ml) was added, and the mixture was heated at 80 °C for 0.5 h. The residue partitioned into *n*-hexane and H₂O, and the *n*-hexane part was analyzed on a GC system equipped with an FID (detector temperature, 300 °C). Chromatography conditions:

injection temperature, 280 °C; column, HP-5 (60 m × 0.32 mm × 0.25 μm); initial column temperature, 200 °C; column temperature increased to 280 °C (10 °C min⁻¹) and kept at 280 °C for 40 min under N₂ carrier gas (1.8 ml min⁻¹).

Animals

Male Kunming mice (16–20 g) were housed for three days prior to use. All animal care and experimental procedures were in accordance with the guidelines of the National Institutes of Health (NIH), and the experimental procedures were approved by the Ethics Committee of Institute of Materia Medica, Chinese Academy of Medical Sciences and Peking Union Medical College (Beijing, China).

Acetic acid-induced writhing tests

Kunming mice (eight per group) were used in the tests. Control mice received 0.9% NaCl (10 ml kg⁻¹, ip), and the test mice received aqueous solutions (10, 3, 1, 0.3, or 0.1 mg kg⁻¹, ip; injection volume: 10 ml kg⁻¹) with a solution concentration of 1 mg ml⁻¹, 0.3 mg ml⁻¹, 0.1 mg ml⁻¹, 0.03 mg ml⁻¹, or 0.01 mg ml⁻¹. Compounds 17–19, 29–31, and 33 utilized 1% Tween 80 as hydrotropic agent. Fifteen minutes later, 1% v/v HOAc solution (0.1 ml/10 g) was administered to the mice by intraperitoneal injection. The number of writhing events for each mouse was counted for 15 min.

Anti-inflammatory activity assays

Compounds were tested for their anti-inflammatory activity by measuring inhibitory effects of LPS-induced NO production in BV2 cells. Curcumin was used as the positive control. The BV2 macrophage cell line was obtained from the Cell Culture Center at the Institute of Basic Medical Sciences, Peking Union Medical College. LPS was bought from Sigma-Aldrich company. After preincubation for 24 h in a 96-well plate, the cells were treated with the test compounds (10⁻⁵ mol L⁻¹), then stimulated with LPS for 24 h. The production of NO was determined *via* measuring the concentration of nitrite in the culture supernatant. NaNO₂ was utilized to generate a standard curve. The absorbances at 550 nm were measured.

Conflicts of interest

The authors declare no competing financial interest.

Acknowledgements

This work was supported by grants from the National Natural Science Foundation of China (No. 21572274, 21732008, and 81630094) and the CAMS Innovation Fund for Medical Sciences (No. 2016-I2M-3-012).

Notes and references

- 1 D. J. Newman and G. M. Cragg, *J. Nat. Prod.*, 2012, 75, 311.
- 2 D. J. Newman and G. M. Cragg, *J. Nat. Prod.*, 2016, 79, 629.



- 3 A. L. Harvey, R. A. Edrada-Ebel and R. J. Quinn, *Nat. Rev. Drug Discovery*, 2015, **14**, 111.
- 4 Chinese Materia Medica Compilation Commission, *Chinese Materia Medica*, 1986, vol. 16. p. 5264.
- 5 Jinan People's Pharmaceutical Factory, *Chin. Tradit. Herb. Drugs*, 1970, **4**, 30.
- 6 Zhaoshanbai Clinical Cooperative Group of Beijing Military Region, *People Mil. Surg.*, 1975, vol. 10, p. 38.
- 7 Xiyang Gaoluo District Hospital, *Shanxi Med. J.*, 1978, **2**, 10.
- 8 Coronary Heart Disease Research Group of Tianjin Institute for Drug Control, *Chin. Tradit. Herb. Drugs*, 1976, **5**, 12.
- 9 Y. Li, Y. B. Liu, J. J. Zhang, Y. Liu, S. G. Ma, J. Qu, H. N. Lv and S. S. Yu, *J. Nat. Prod.*, 2015, **78**, 2887.
- 10 Y. X. Zhu, Z. X. Zhang, H. M. Yan, D. Lu, H. P. Zhang, L. Li, Y. B. Liu and Y. Li, *J. Nat. Prod.*, 2018, **81**, 1183.
- 11 C. S. Niu, Y. Li, Y. B. Liu, S. G. Ma, L. Li, J. Qu and S. S. Yu, *Tetrahedron*, 2016, **72**, 44.
- 12 C. S. Niu, Y. Li, Y. B. Liu, S. G. Ma, F. Liu, S. Xu, X. J. Wang, S. Liu, R. B. Wang, J. Qu and S. S. Yu, *RSC Adv.*, 2017, **69**, 43921.
- 13 N. Sun, Y. Zhu, H. F. Zhou, J. F. Zhou, H. Q. Zhang, M. K. Zhang, H. Zeng and G. M. Yao, *J. Nat. Prod.*, 2018, **81**, 2673.
- 14 N. Sun, Y. Qiu, J. J. Liu, H. Q. Zhang, Q. H. Zhang, M. K. Zhang, G. J. Zheng, C. Zhang and G. M. Yao, *Phytochemistry*, 2019, **158**, 1.
- 15 X. C. Li, D. Ferreira and Y. Q. Ding, *Curr. Org. Chem.*, 2010, **14**, 1678.
- 16 L. Q. Wang, S. N. Chen, K. F. Chen, C. J. Li and G. W. Qin, *Phytochemistry*, 2000, **54**, 847.
- 17 T. Kaiya and J. Sakakibara, *Chem. Pharm. Bull.*, 1985, **33**, 4637.
- 18 M. K. Zhang, Y. Y. Xie, G. Q. Zhan, L. Lei, P. H. Shu, Y. L. Chen, Y. B. Xue, Z. H. Luo, Q. Wan, G. M. Yao and Y. H. Zhang, *Phytochemistry*, 2015, **117**, 107.
- 19 J. Sakakibara, N. Shirai, T. Kaiya and H. Nakata, *Phytochemistry*, 1979, **18**, 135.
- 20 L. Q. Wang, B. Y. Ding, W. M. Zhao and G. W. Qin, *Chin. Chem. Lett.*, 1998, **9**, 465.
- 21 J. W. Burke and R. W. Duskotch, *J. Nat. Prod.*, 1990, **53**, 131.
- 22 J. Sakakibara, N. Shirai, T. Kaiya and Y. Litaka, *Phytochemistry*, 1980, **19**, 1495.
- 23 S. F. Elnaggar, R. W. Duskotch, T. M. Odell and L. Girard, *J. Nat. Prod.*, 1980, **43**, 617.
- 24 T. Ohta and H. Hikino, *Magn. Reson. Chem.*, 2010, **12**, 445.
- 25 J. Katakawa, T. Tetsumi, T. Terai, M. Katai, K. Sakaguchi and M. Sato, *J. Chem. Crystallogr.*, 2000, **30**, 573.
- 26 H. Hikino, T. Ohta, S. Koriyama, Y. Hikino and T. Takemoto, *Chem. Pharm. Bull.*, 1971, **19**, 1289.
- 27 I. Sakamoto, K. Yamasaki and O. Tanaka, *Chem. Pharm. Bull.*, 2008, **25**, 3437.
- 28 J. W. Burke, R. W. Duskotch, C. Z. Ni and J. Clardy, *J. Am. Chem. Soc.*, 1988, **111**, 5831.
- 29 J. Sakakibara, N. Shirai and T. Kaiya, *Phytochemistry*, 1981, **20**, 1744.
- 30 Y. Li, Y. X. Zhu, Z. X. Zhang, Y. L. Liu, Y. B. Liu, J. Qu, S. G. Ma, X. J. Wang and S. S. Yu, *Tetrahedron*, 2018, **74**, 693.
- 31 X. Li, Y. F. Liu, K. M. Ye, W. X. Yuan and Y. J. Han, *J. Shenyang Pharm. Univ.*, 1978, **9**, 17.
- 32 F. Y. Fu, Y. Z. Zhang, T. M. Shang, S. R. Luo, B. Y. Zhang and Z. J. Wang, *Chin. Pharm. J.*, 1980, **15**, 13.
- 33 S. Hara, H. Okabe and K. Mihashi, *Chem. Pharm. Bull.*, 1981, **35**, 501.

